Impact of Energy Storage on Renewable Energy Utilization: A Geometric Description

Zhongjie Guo, Wei Wei, *Senior Member, IEEE*, Laijun Chen, *Senior Member, IEEE*,
Zhao Yang Dong, *Fellow, IEEE*, and Shengwei Mei, *Fellow, IEEE*

Abstract—The high penetration of volatile renewable energy challenges power system operation. Energy storage units (ESUs) can shift the demand over time and compensate real-time discrepancy between generation and demand, and thus improve system operation flexibility and reduce renewable energy curtailment. This paper proposes two parametric optimization models to quantify how the power (MW) and energy (MWh) capacity of ESU would impact renewable energy utilization from two aspects: renewable energy curtailment and system flexibility for uncertainty mitigation. The two indicators are characterized as multivariate functions in the capacity parameters of ESUs. A severity ranking algorithm is suggested to pick up critical scenarios of fluctuation patterns from the uncertainty set; consequently, the proposed models come down to multi-parametric mixed-integer linear programs (mp-MILPs) which can be solved by a decomposition algorithm. The proposed method provides analytical expressions of the two indicators as functions in MW and MWh capacity. Such a characterization delivers abundant sensitivity information on the impact of ESU capacity parameters, and provides a powerful tool for visualization and useful reference for storage sizing. Case studies verify the effectiveness of the proposed method and demonstrate how to use the geometric information.

Index Terms—Energy storage unit, flexibility, renewable generation, uncertainty, visualization.

NOMENCLATURE

A. Indices and Sets

$i \in \mathbb{G}$	Index of generators in set $\mathbb{G}$.
$j \in \mathbb{S}$	Index of energy storage units in set $\mathbb{S}$.
$k \in \mathbb{W}$	Index of renewable plants in set $\mathbb{W}$.
$q \in \mathbb{D}$	Index of loads in set $\mathbb{D}$.
$l \in \mathbb{L}$	Index of transmission lines in set $\mathbb{L}$.
$t \in \mathbb{T}$	Index of time periods in set $\mathbb{T}$.
Θ	Parameter set.
Ξ	Uncertainty set.

B. Parameters

p_{qt}^d	Demand at load bus q in period t.
F_l	Power flow limit of transmission line l.
p_i^{gn}/p_i^{gm}	Minimum/maximum output of generator i.
R_i^+/R_i^-	Upward/downward ramp limit of generator i.
η_j^c/η_j^d	Charging/discharging efficiency of ESU j.
E_{j0}^s	Initial state-of-charge of ESU j.
p_{kt}^{rm}	Dispatchable power of plant k in period t.
ξ	Vector of uncertain parameters.
ξ_0	Vector of predicted renewable power output.
h	Vector of forecast errors.

C. Variables

p_{it}^g	Output of generator i in period t.
p_{jt}^{sc}	Charging power of ESU j in period t.
p_{jt}^{sd}	Discharging power of ESU j in period t.
p_{kt}^r	Dispatched power of plant k in period t.
Δp_{kt}^r	Curtailed power of plant k in period t.
b_{jt}^s	Status indicator of ESU j in period t.
p_j^{sm}/E_j^m	Power/Energy capacity of ESU j.
$\Delta \xi$	Vector of renewable energy curtailment.

I. INTRODUCTION

DURING the past decade, the excessive consumption of fossil fuels, global warming, and environmental deterioration have promoted the rapid development of renewable energy generation (REG) [1]. However, the growing penetration of volatile REG has exerted challenges on power system operation [2]. On the one hand, wind power is difficult to predict accurately, and the solar panel produces no power during the night. On the other hand, the variation tendency of REG does not follow that of the load [3]. As a result, although a large capacity of REG has been installed to meet the demand over certain periods, excessive renewable power is curtailed when the load is insufficient or the transmission line is congested, causing a waste of energy and a low utilization rate of facility, for example, in the northwest provinces of China [4].

Deploying energy storage units (ESU) has been acknowledged as the most effective solution of supporting grid integration of large-scale renewable energy: ESU can compensate the real-time discrepancy between generation and demand and shift the net demand over time, and therefore help mitigate the uncertainty of REGs [5], [6], improve security margin [7], [8], and reduce the operating cost [9], [10].

In view of the appealing feature of ESU, extensive work has been carried out to investigate the impact that ESU can exert on renewable energy utilization. In renewable abundant areas, cutting down renewable energy curtailment is one of the main considerations in ESU planning and operation [11]. A two-stage optimization problem is developed in [12] to determine the capacity of battery energy storage, which aims to reduce wind energy curtailment in wind farms; the curtailment is penalized in the objective function. A scenario-based two-stage ESU planning framework is proposed in [13]; the first stage determines the capacity of ESU; the second stage optimizes the strategy to reduce the expected daily cost. In [14], the potential of pumped storage on maximizing the wind energy utilization is explored. Energy storage is also expected to improve the operational economy in unit commitment (UC) and energy dispatch, given the fact that startup and shutdown of generating units are less frequently as the gap between peak and valley demands shrinks. A stochastic UC is formulated in [15] to deal with the uncertainty of REG, considering ideal and generic ESUs. In systems with high levels of renewable resources, energy storage supports conventional generators to increase the short-term profitability as ESU can store and shift clean energy and has fast ramping capability [9].

Except for shaving peak demand and reducing renewable energy curtailment, another crucial role of ESU is to offer short-term backup for mitigating the uncertainty of REGs [16]; as a controllable device, ESU is actually able to provide additional flexibility to compensate unavoidable real-time mismatches between the production and consumption of electricity [17]; hence the system reliability is enhanced. In [18], the ability of energy storage systems to provide contingency reserve is explicitly modeled in a security-constrained UC problem; the energy storage can compensate the power inadequacy caused mainly by ramping limits of thermal generators. The work in [19] aims to provide a systematic approach to qualify the level of flexibility of a power system, which helps address deviations in variable REG; an online index is considered to evaluate the technical aptitude of the fast ramping units, hourly demand response, and energy storage systems to deliver the required flexibility. In [20], electric and thermal storage in a multi-energy community are used to provide extra demand response flexibility; the multi-energy formulation allows comprehensive modeling of different flexibility options and thus guarantees the robustness against any operation call. More work is introduced in [21]–[23] to address the issue of operational reliability and adequacy of power systems with ESUs, considering a high penetration level of REGs and the fast fluctuations of wind power.

Indubitably, the impact on renewable energy utilization provided by ESU largely depends on its charging/discharging power capacity (in MW) and energy capacity (in MWh). In the existing work, the attention has been paid to the energy capacity, while the power capacity is assumed to be proportional according to a ratio, such as in [24], [25]. Furthermore, the evaluation in the current work entails a sampling-based framework: an optimization problem is solved with multiple sampled parameters, a representative case is [13]. Although this popular framework offers a general trend on the system impact of specific parameters, it does not offer any analytical sensitivity information and structured property of the optimal value as a function of parameters under investigation. Such quantitative information is desired to help decision making in practice. In this regard, this paper aims to develop a thorough method that discloses the impact of ESU on renewable energy utilization and operation flexibility as analytical functions in power and energy capacity parameters, providing the decision-maker a holistic landscape of possible outcomes as well as a useful tool for visualization.

The main contributions are twofold:

1) We propose two parametric optimization models to quantify the impact of ESU on two indicators: renewable energy curtailment and system flexibility for mitigating fluctuation of REG. The volatility of REG is described by an uncertainty set built with predicted output and forecast errors, and the models are parameterized in the power and energy capacities of ESUs. In the first model, we calculate the total amount of renewable energy curtailment in the worst-case scenario, giving rise to a parametric max-min problem. In the second model, a scalar variable, which determines the size of uncertainty set and reflects the level of REG volatility, is maximized on condition that the dispatch constraints remain feasible given any scenario from the uncertainty set; such a scalar measures the system's capability to mitigate uncertainty.

2) We develop a computationally viable method to transform the parametric robust optimization models into canonical multi-parametric mixed-integer linear programs (mp-MILPs). Based on the extreme property of the worst-case scenario, we propose a severity ranking algorithm to pick up only critical scenarios of fluctuation patterns from the uncertainty set. Then, by considering these critical scenarios, the parametric models are transformed to mp-MILPs with moderate sizes, which can be solved by a heuristic decomposition algorithm. The outcomes describe the two indicators as explicit functions in ESU capacity parameters. The proposed method is tested on the modified IEEE 9-bus system and IEEE 118-bus system, validating the effectiveness of the geometric characterization. Visualization results demonstrate the information delivered by the proposed method and how such outcomes can help decision making in practice.

The rest of this paper is organized as follows: the concrete model of power system operation with REGs and ESUs is introduced in Section II, followed by the parametric robust optimization models of the two indicators based on the compact matrix forms. The solution methodology is developed in Section III. Case studies and analysis are presented in Section IV. Conclusions are drawn in Section V.

II. Mathematical Formulation

The concrete model of power system operation with ESUs and REGs is introduced; then, the parametric robust optimization models are set forth based on the compact matrix form.

A. Multi-Period Economic Dispatch

Since this paper concerns with renewable utilization and system flexibility relevant targets, the operation constraints are presented first without an economic objective function. The power transmission network is modeled via the renowned direct-current power flow. Then, power system operation with ESU is cast as a multi-period dynamic dispatch including the following constraints:

$$\sum_{i\in\mathbb{G}} p_{it}^g + \sum_{j\in\mathbb{S}}(p_{jt}^{sd} - p_{jt}^{sc}) + \sum_{k\in\mathbb{W}} p_{kt}^r = \sum_{q\in\mathbb{D}} p_{qt}^d, \forall t \quad (1a)$$

$$-F_l \le \sum_{i\in\mathbb{G}} \pi_{li} p_{it}^g + \sum_{j\in\mathbb{S}} \pi_{lj}(p_{jt}^{sd} - p_{jt}^{sc})$$
$$+ \sum_{k\in\mathbb{W}} \pi_{lk} p_{kt}^r - \sum_{q\in\mathbb{D}} \pi_{lq} p_{qt}^d \le F_l, \forall l \in \mathbb{L}, \forall t \quad (1b)$$

$$p_i^{gn} \le p_{it}^g \le p_i^{gm}, -R_i^- \le p_{it+1}^g - p_{it}^g \le R_i^+, \forall i \in \mathbb{G}, \forall t \quad (1c)$$

$$0 \le p_{jt}^{sc} \le b_{jt}^s p_j^{sm}, 0 \le p_{jt}^{sd} \le (1-b_{jt}^s)p_j^{sm}, \forall j \in \mathbb{S}, \forall t \quad (1d)$$

$$\alpha_j^l E_j^m \le E_{j0}^s + \sum_{\tau=1}^t (p_{jt}^{sc}\eta_j^c - p_{jt}^{sd}/\eta_j^d) \le E_j^m, \forall j \in \mathbb{S}, \forall t \quad (1e)$$

$$0 \le p_{kt}^r \le p_{kt}^{rm}, \forall k \in \mathbb{W}, \forall t \quad (1f)$$

where (1a) is the system-wide power balancing condition; (1b) stipulates the power flow limits in transmission lines where $\pi_{l(\cdot)}$ denotes the power transfer distribution factor (PTDF) from an arbitrary facility $(\cdot)$ to line l. (1c) restricts the output and ramping rates of generators. (1d) imposes complementarity constraints on charging and discharging power where $b_{jt}^s = 1$ for charging and $b_{jt}^s = 0$ for discharging; the charging power and discharging power can be 0 at the same time, regardless of the value of b_{jt}^s. (1e) confines the state-of-charge (SoC) dynamics of ESU where α_j^l is the lower bound coefficient of SoC level. E_{j0}^s is the initial level of SoC; sometimes, the terminal SoC E_{jT}^s is set to the initial state E_{j0}^s in order to complete a cycle. (1f) prescribes the maximum dispatchable power of a renewable plant p_{kt}^{rm}, which is an uncertain parameter and depends on the weather condition; the dispatched power p_{kt}^r cannot exceed p_{kt}^{rm}, and renewable energy curtailment is $\Delta p_{kt}^r = p_{kt}^{rm} - p_{kt}^r$. In the rest of this paper, we eliminate dispatched power p_{kt}^r by replacing it with $p_{kt}^{rm} - \Delta p_{kt}^r$ and constraint $0 \le \Delta p_{kt}^r \le p_{kt}^{rm}$ where the curtailment Δp_{kt}^r is regarded as an independent decision variable.

It is necessary to impose complementarity on charging and discharging power. In an economic operation problem, charging and discharging power are naturally complementary, as analyzed in [26], as simultaneous charging and discharging are not optimal due to losses. In contrast, in the renewable energy curtailment problem, simultaneous charging and discharging can act as a load that consumes excessive renewable energy and thus reduce the curtailment, so complementarity must be enforced via binary variables.

With regard to the power flow model, the DC network model is generally a satisfactory approximation in transmission systems and is widely used in related literature such as [14], [27]. Nevertheless, to consider the nodal voltage and reactive power in the network power flow formulation, the model developed in [28] can be used, which remains linear, and thus will not jeopardize the implementation of the method to be proposed.

Before proceeding to the compact model, the above constraints have to be revamped because of the specific technique used in this paper. First, the only equality constraint (1a) can be eliminated by expressing the output of the slack generator using remaining variables; or, it can be replaced by two opposite inequalities. If the constraint $E_{j0}^s = E_{jT}^s$ is considered, it also can be replaced by $E_{j0}^s \le E_{jT}^s$ and $E_{j0}^s \ge E_{jT}^s$. Moreover, although p_j^{sm} is fixed in the operation problem, it will be treated as a varying parameter in the parametric model. Hence, the product $b_{jt}^s p_j^{sm}$ in (1d) is bilinear. By introducing a continuous variable v_{jt}^s with the following constraints:

$$0 \le v_{jt}^s \le Mb_{jt}^s, 0 \le p_j^{sm} - v_{jt}^s \le M(1-b_{jt}^s), \forall j \in \mathbb{S}, \forall t \quad (2)$$

where M is a large enough constant, the relation $v_{jt}^s = b_{jt}^s p_j^{sm}$ must hold as b_{jt}^s is either 0 or 1.

In order to characterize the impact of ESU capacity parameters, we encapsulate $p_j^{sm}, \forall j$ (MW) and $E_j^m, \forall j$ (MWh) into a vector θ; specifically, we use ξ and $\Delta\xi$ to denote the weather-dependent renewable power p_{kt}^{rm} which is uncertain and the curtailed renewable power $\Delta p_{kt}^r, \forall k \in \mathbb{W}, \forall t$. All the remaining continuous variables, including the auxiliary variable v_{jt}^s, and discrete ones, are enclosed into vectors x and y, respectively. All constraints in (1) and (2) can be written in the following linear inequality form parameterized in θ:

$$Ax + By + C(\xi - \Delta\xi) \le b + F\theta \quad (3)$$

where A, B, C, b and F are constant coefficients. The storage capacity parameter takes values in the following parameter set

$$\Theta = \{\theta | S\theta \le H\} \quad (4)$$

Θ is a polyhedron and defines the concerned range of θ subject to technical and economic considerations. Taking the investment cost for an example, the capital cost of ESU j can be expressed as $s_1 p_j^{sm} + s_2 E_j^m$; the first term pertains to the cost of power electronics converters, and the second one the cost of battery array. Given an available budget H_0, a linear inequality $s_1 p_j^{sm} + s_2 E_j^m \le H_0$ is added in the parameter set.

B. Uncertainty Set

Akin to robust optimization methods [29], [30], the weather-dependent parameter ξ resides in a cardinality-constrained uncertainty set:

$$\Xi = \{\xi | \xi = \xi_0 + \alpha(z^+ - z^-) \cdot h, \ (z^+, z^-) \in Z\} \quad (5)$$

where

$$
Z = \left\{ (z^+, z^-) \left| \begin{array}{l} z^+, z^- \in \{0, 1\}^{N_\xi} \\ z^+ + z^- \leq \mathbf{1} \\ \mathbf{1}^\top (z^+ + z^-) \leq \Gamma \end{array} \right. \right\} \tag{6}
$$

where $\xi_0 \in \mathbb{R}^{N_\xi}$ is the predicted REG output with a dimension of N_ξ, which relates to the number of time periods and renewable plants; constant vector $h \in R^{N_\xi}$ represents forecast errors; symbol $\cdot$ denotes the element-wise product of two vectors with the same dimension; α is a nonnegative scaling factor, reflecting the accuracy of prediction; a larger α implies a less accurate prediction and a more conservative uncertainty set; $\Gamma < N_\xi$ is called the budget of uncertainty, implying that at most Γ elements in ξ can reach their lower or upper bounds. The symbol $\mathbf{1}$ is an all-one column vector with a compatible dimension.

It is important to investigate how the parameter θ would impact system operation with uncertain REG. In what follows, two indicators are proposed. One is the renewable energy curtailment; the other measures how much uncertainty can be mitigated using available generation assets.

C. Impact of ESU on Renewable Energy Curtailment

Consider the following parametric max-min problem

$$
v_c(\theta) = \max_{\xi \in \Xi} \min_{x, y, \Delta\xi} \mathbf{1}^\top \Delta\xi
$$
$$
\text{s.t. } Ax + By + C(\xi - \Delta\xi) \leq b + F\theta \tag{7}
$$
$$
\Delta\xi \geq 0
$$

Problem (7) aims to find a dispatch strategy that leads to the minimum renewable energy curtailment in the worst-case scenario that resides in the uncertainty set Ξ with $\alpha = 1$ (here we assume the vector $\mathbf{1}$ has a unit of hour). For any given θ, the optimal value function is $v_c(\theta)$.

Because the element in Ξ is finite, the max operator in (7) comes down to enumerating all the elements belonging to Ξ in the epigraph formulation [31], yielding:

$$
v_c(\theta) = \min_{x_i, y_i, \lambda, \Delta\xi_i} \lambda
$$
$$
\text{s.t. } Ax_i + By_i + C(\xi_i - \Delta\xi_i) \leq b + F\theta, \forall i \tag{8}
$$
$$
\xi_i = \xi_0 + (z_i^+ - z_i^-) \cdot h
$$
$$
\lambda \geq \mathbf{1}^\top \Delta\xi_i, \Delta\xi_i \geq 0, \forall i
$$

where $\{\xi_i\}, \forall i$ are the elements of Ξ; for each ξ_i, the response of the power system includes generation redispatch x_i, y_i and REG curtailment $\Delta\xi_i$.

Problem (8) is an mp-MILP. Basically, we need to solve it for the explicit expression of $v_c(\theta)$. The solution methodology will be presented later in Section III.

D. Impact on Uncertainty Mitigation

One crucial role of ESU is to compensate the uncertainty of REG without violating network operating constraints (1). To quantify the impact of θ on uncertainty mitigation, consider the following feasibility problem:

$$
\forall \xi \in \Xi(\alpha), \exists x, y, \Delta\xi \geq 0 :
$$
$$
Ax + By + C(\xi - \Delta\xi) \leq b + F\theta \tag{9}
$$

Condition (9) requires the existence of at least one redispatch strategy regardless of the value of $\xi \in \Xi(\alpha)$ [32], [33]. In contrast to the previous indicator in which α is fixed, the term αh in (5) measures how far the renewable power can deviate from the prediction by incorporating variable α, which reflects the level of uncertainty. If condition (9) is satisfied with bigger α, the power system enjoys higher flexibility to mitigate uncertainty, leading to the following model that maximizes the ability of uncertainty mitigation:

$$
v_f(\theta) = \max_{x_i, y_i, \alpha, \Delta\xi_i} \alpha
$$
$$
\text{s.t. } Ax_i + By_i + C(\xi_i - \Delta\xi_i) \leq b + F\theta, \forall i
$$
$$
\xi_i = \xi_0 + \alpha(z_i^+ - z_i^-) \cdot h, \forall (z_i^+, z_i^-) \in Z \tag{10}
$$
$$
\alpha \geq 0, \Delta\xi_i \geq 0, 0 \leq \xi_i \leq C^r, \forall i
$$

Similarly to (8), $\{\xi_i\}, \forall i$ are all elements of $\Xi(\alpha)$; nevertheless, the magnitude of ξ is proportional to α and bounded by the installed capacity of renewable plant as in the last constraint of (10). The enumeration index is actually associated with the elements in Z. Again, problem (10) is an mp-MILP.

Since renewable curtailment is allowed, (9) is always feasible when the REG rises as long as the traditional generators have enough capacity; thus, the optimal value of (10) is determined by the backup sufficiency when the demand grows but REG drops down. On the contrary, the first indicator guarantees that excessive REG can be used when the demand decreases while the REG increases. Therefore, the two indicators complement each other.

III. SOLUTION METHODOLOGY

The geometric characterization of the impact of ESU capacity parameters calls for solving mp-MILPs (8) and (10). However, the direct enumeration of the elements in the uncertainty set is not computationally viable. This section proposes a scenario ranking algorithm to pick up a pre-specified number of critical scenarios from Ξ. Then, the reduced mp-MILPs can be solved with moderate computational efforts.

A. Ranking of Critical Scenarios

Although uncertainty set Ξ has a large number of elements, only a small fraction would impact the solution, and most scenario-dependent constraints in (8) and (10) are redundant, causing computational overhead. In this regard, we can rank the scenarios according to their influence on the optimal values of (8) and (10). The flowchart is summarized in Algorithm 1.

Indeed, Algorithm 1 gives the relative ranking of fluctuation patterns $(z^+, z^-) \in Z$. Such a ranking is mainly influenced by the generator ramping parameter and load profile. If pattern A

Algorithm 1: Scenario Ranking.

1: Initiate $\Xi_C = \emptyset$; fix $\theta = 0$, $\alpha = 1$; specify a required number of critical scenarios N_C; iteration index $K = 0$.

2: Solve the specialized subproblem discussed in subsections B and C; the optimal solution is ξ^*, $z^* = \{z^{+*}, z^{-*}\}$; update $\Xi_C = \Xi_C \cup \{\xi^*\}$.

3: If $K = N_C$, terminate and report Ξ_C. Otherwise update $K \leftarrow K + 1$; add a cut $\|z - z^*\|_2^2 \geq 1$ into the subproblem and go to step 2.

---

is more severe than pattern B for $\theta = 0$, then it is not difficult to believe A remains more severe than B for other values of θ; although both patterns may have less impact when the storage capacity grows, their relative ranking does not change. Hence, we choose $\theta = 0$ in Algorithm 1, so that storage operation constraints vanish, and the operation problem becomes linear. A validation on this algorithm is given in Section IV-A4.

B. Subproblem of Renewable Energy Curtailment

For renewable energy curtailment problem (8), the subproblem refers to problem (7); the optimal solution ξ^* consists of a fluctuation pattern $z^* = \{z^{+*}, z^{-*}\}$ which causes maximum renewable energy curtailment and thus is picked up as a critical scenario. As we fix $\theta = 0$ in step 1, storage constraints as well as binary variables stipulating complementary charging/discharging are excluded, so problem (7) comes down to a linear max-min problem

$$\max_{\xi \in \Xi} \ \min_{x, \Delta\xi} \ \mathbf{1}^\top \Delta\xi$$

$$\text{s.t.} \quad Ax + C(\xi - \Delta\xi) \leq b : \beta$$

$$\xi = \xi_0 + (z^+ - z^-) \cdot h, \Delta\xi \geq 0 \quad (11)$$

where β after the colon is the vector of dual variables of the inner minimization problem. Taking the dual of the inner linear program, problem (11) can be cast as a bilinear program [34] as follows

$$\max_{\xi \in \Xi, \beta} \ \beta^\top b - \beta^\top C\xi$$

$$\text{s.t.} \quad A^\top \beta = 0, -C^\top \beta \leq \mathbf{1}$$

$$\beta \leq 0, \xi = \xi_0 + (z^+ - z^-) \cdot h \quad (12)$$

The constraints of problem (12) are linear, but there is a product term $\beta^\top C\xi$, which is bilinear, in the objective function. Expanding $\beta^\top C\xi$ in an element-wise form [29]:

$$\beta^\top C\xi = \beta^\top C\xi_0 + \sum_i \sum_j c_{ij}\beta_i(z_j^+ - z_j^-)h_j \quad (13)$$

where c_{ij} is the element of matrix C. Then, $\beta_i z_j^+$ and $\beta_i z_j^-$ involving the product of a continuous variable and a binary variable can be replaced by u_{ij}^+ and u_{ij}^- together with a set of

linear constraints; and (12) is equivalently transformed into

$$\max \ \beta^\top b - \beta^\top C\xi_0$$

$$- \sum_i \sum_j c_{ij}(u_{ij}^+ - u_{ij}^-)h_j$$

$$\text{s.t.} \quad A^\top \beta = 0, -C^\top \beta \leq \mathbf{1}, \beta \leq 0$$

$$M(z_j^+ - 1) \leq \beta_i - u_{ij}^+ \leq 0, \forall i, j$$

$$- Mz_j^+ \leq u_{ij}^+ \leq 0, \forall i, j$$

$$M(z_j^- - 1) \leq \beta_i - u_{ij}^- \leq 0, \forall i, j$$

$$- Mz_j^- \leq u_{ij}^- \leq 0, \forall i, j$$

$$z^+, z^- \in \{0, 1\}^{N_\xi}, z^+ + z^- \leq 1$$

$$\mathbf{1}^\top(z^+ + z^-) \leq \Gamma$$

$$\text{hole cuts } (z, z_k^*), \ k = 1 : K \quad (14)$$

where M is a large enough constant. The last constraint precludes critical scenarios z_k^* obtained in the previous iterations. To see this, the quadratic constraint $\|z - z_k^*\|_2^2 \geq 1$ creates a hole around z_k^* [35]. Because z is binary and $z_i^2 = z_i$ always holds, the hole cuts finally reduce to linear constraints

$$\sum_i (z_i + z_{ki}^* - 2z_i z_{ki}^*) \geq 1, \ k = 1, \ldots, K \quad (15)$$

Now, the subproblem of renewable energy curtailment comes down to MILP (14), which is readily solvable.

C. Subproblem of Uncertainty Mitigation

In the uncertainty mitigation problem, renewable volatility aims to damage the feasibility of operation constraints. We introduce a vector s of slack variables measuring potential constraint violations, and build the following feasibility check subproblem:

$$\max_{\xi \in \Xi} \ \min_{x, y, \Delta\xi, s} \ \mathbf{1}^\top s$$

$$\text{s.t.} \ Ax + C(\xi - \Delta\xi) - s \leq b$$

$$\xi = \xi_0 + (z^+ - z^-) \cdot h \quad (16)$$

$$s \geq 0, \Delta\xi \geq 0$$

The slack variables s can be viewed as emergency control, such as load shedding, to prevent the system from failure; the uncertain REG ξ tries to bring the largest damage to the system, while the operator endeavors to minimizes the loss subject to the value of ξ. Thus, the optimal solution ξ^* of (16) is deemed to be the critical scenario in the uncertainty mitigation problem. Note that the members in family $\{\Xi(\alpha)\}, \forall \alpha$ share the same shape, and they only differ in size, so the critical fluctuation pattern $z = \{z^+, z^-\}$ better captures the essence of an extreme event. In this regard, we fix $\alpha = 1$ in (16). The linear max-min problem (16) has the same structure as (11), so it can be reformulated as an MILP in the similar way.
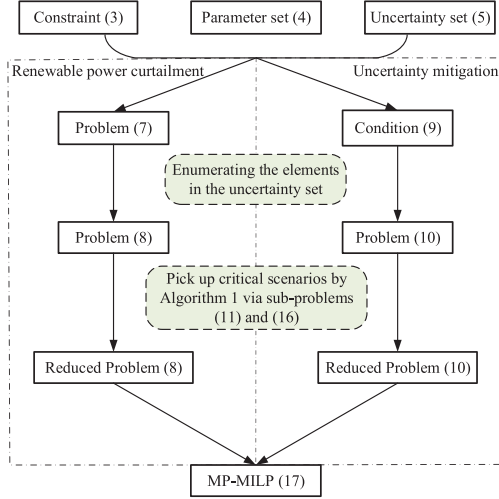
Fig. 1.   Flowchart of modeling and reformulation in Sections II and III.

D. The Final mp-MILP

The modeling and solution are summarized in the flowchart in Fig. 1. By Algorithm 1, a total number N_C of critical scenarios in the renewable energy curtailment problem or the uncertainty mitigation problem have been picked out. Then, mp-MILPs (8) and (10) with moderate sizes can be set up in the standard form

$$
\begin{aligned}
v(\theta) = \min_{x_p, y_p} \ & c_p^\top x_p \\
\text{s.t. } & A_p x_p + B_p y_p \leq b_p + F_p \theta \\
& \theta \in \Theta
\end{aligned}
\tag{17}
$$

where x_p and y_p are vectors of continuous and discrete variables; A_p, B_p, b_p and F_p are constant coefficients.

We employ the method proposed in [36] to solve (17), which basically consists of 4 steps:

1) We first solves MILP (17) by treating θ as a decision variable, and determines the binary variable y_{p0}^*.

2) Given $y_p = y_{p0}^*$ and $\theta \in \Theta$, mp-MILP (17) degenerates into the following mp-LP:

$$
\begin{aligned}
v_0(\theta) = \min_{x_p} \ & c_p^\top x_p \\
\text{s.t. } & A_p x_p \leq (b_p - B_p y_{p0}^*) + F_p \theta \\
& \theta \in \Theta
\end{aligned}
\tag{18}
$$

(18) can be solved by POP toolbox [37]; the solution consists the piecewise linear optimal value function (OVF) $v_0(\theta)$ and N_0 critical regions (CRs); CR_i is a subset of Θ, whose corresponding piece of OVF $v_0^i(\theta)$ remains optimal with any point in this CR. Besides, $\Theta = \cup_{i=1}^{N_0} \mathrm{CR}_i$.

3) Then, for any $\mathrm{CR}_i, i = 1, \ldots, N_0$ with the currently corresponding piece of OVF $v_0^i(\theta)$, an MILP problem is formulated to check if there is any other solution of y_p than achieves a lower

optimal value, i.e.

$$
\begin{aligned}
v_0(\theta) = \min_{x_p, \theta} \ & c_p^\top x_p \\
\text{s.t. } & A_p x_p + B_p y_p \leq b_p + F_p \theta \\
& \theta \in CR_i, c_p^\top x_p \leq v_0^i(\theta) \\
& \|y_p - y_{p0}^*\|_2^2 \geq 1
\end{aligned}
\tag{19}
$$

where the cut $\|y_p - y_{p0}^*\|_2^2 \geq 1$ excludes y_{p0}^*, and can be linearized as the hole cus in (14); it multiplies as the iteration progress to exclude all the binary solutions involved in the current CR_i. If (19) is feasible, the optimal solution y_{p1}^{i*} is saved; with $y_p = y_{p1}^{i*}$ and $\theta \in \mathrm{CR}_i$, we can build an mp-LP problem (18), whose OVF is $v_1^{i*}(\theta)$. Consequently, the point-wise minimizing comparison between $v_0^i(\theta)$ abd $v_1^{i*}(\theta)$ is conducted, giving rise to $v_1^i(\theta)$.

By checking all $\mathrm{CR}_i, i = 1, \ldots, N_0$, the updated solution of mp-MILP (17) consists of N_1 CRs and the OVF $v_1(\theta)$, which has N_1 linear pieces $v_1^i(\theta), i = 1, \ldots, N_1$. Here completes the first iteration.

4) Iteratively, we can go back to step 3 with CR_i and $v_1^i(\theta), i = 1, \ldots, N_1$; after k iterations, the algorithm terminates because (19) is infeasible for all $\mathrm{CR}_i, i = 1, \ldots, N_k$, which implies no new binary variable can be found to attain a lower optimal value. The final solution of mp-MILP (17) includes N_k CRs and the corresponding pieces of OVF $v_k(\theta)$, i.e.

$$
v(\theta) = v_k(\theta) = \begin{cases} \mu_1 + \nu_1^\top \theta, & \theta \in CR_1, y = y_1 \\ \vdots & \vdots \\ \mu_{N_k} + \nu_{N_k}^\top \theta, & \theta \in CR_{N_k}, y = y_{N_k} \end{cases}
\tag{20}
$$

where μ_i and ν_i are coefficients of OVF. Therefore, the parameterized expressions of (20) can explicitly reveal the impact of ESU capacity parameters. More importantly, the coefficients ν_i and μ_i carry analytical sensitivity information that traditional sampling methods cannot provide.

More detailed discussion on this method can be found in [36].

IV. CASE STUDIES

Numeric tests on the modified IEEE 9-bus system and IEEE 118-bus system are conducted. Historical data in four typical days, one in each season, are selected to build the renewable generation curve and uncertainty set, so $N^\xi = 96\|\mathbb{W}\|$; the weather data in Qinghai Province, China are used [38]; the uncertainty budget Γ is set to $20\|\mathbb{W}\|$; the forecast error h is set to 20% of the nominal value ξ_0 referring to [39]. Besides, the initial level of SoC is set to 50% of energy capacity; η^c / η^d is 90%.

In Algorithm 1, $N_C = 5$ is used; a brief explanation about the choice of N_C is given below: taking the renewable energy curtailment, problem (7) is actually the second stage in a two-stage robust optimization problem, whose typical form is

$$
\min_{y \in Y} c^\top y + \max_{\xi \in \Xi} \min_{x \in F(y, \xi)} b^\top x
$$

where y is the first-stage decision variable; after y is determined, the uncertain variable ξ seeks a strategy that can maximize the second-stage cost in the uncertainty set Ξ; x is the second-stage decision variable in response to ξ, and its feasible region is $F(y, \xi) = \{x : Gx \geq h - Ey - M\xi\}$. The two-stage robust optimization model is a well-studied topic. More details can be found in [40].

To solve such a two-stage robust problem, column and constraint generation (CCG) algorithm is employed. In this algorithm, a set of significant scenarios of ξ is identified by iterations to cover the worst case ξ^*. In our paper, the critical scenarios essentially paly a similar role as the identified scenarios do in CCG algorithm; they are expected to cover the worst case ξ^* given any parameter of storage capacity. In [40], the performance test on CCG algorithm indicates that the number of significant scenarios defining the worst case cost is relatively stable and small, regardless of the problem size and uncertainty budget. Meanwhile, this number generally varies from 4 to 6. Given this, we set $N_c = 5$ in this paper.

Optimization problems are solved by CPLEX 12.6 on a laptop with Intel i5-8250 U CPU and 8 GB memory.

### A. 9-Bus System With a Single ESU

A wind farm with 180MW installed capacity and an ESU connect to the system at Bus 4. Referring to the typical data of lead-acid battery used in [41], we set the power and energy capacity cost coefficients to $s_1 = 3 \times 10^5$\$/MW and $s_2 = 2 \times 10^5$\$/ MWh, respectively; the budget $H_0 = 3 \times 10^7$\$. All the data directly used in the tests can be found in [42].

1) Results on Renewable Energy Curtailment: The optimal value function $v_c(\theta)$ is visualized in Fig. 2(a), showing the significant impact of ESU on renewable energy curtailment. The bottleneck that prevents effective utilization of wind energy is the generation-demand mismatch, like the late-night hours when the wind energy is rich while the demand is low. Without ESU, the wind energy curtailment is as high as 52.9 MWh. Projecting the pieces of $v_c(\theta)$ onto the parameter space, the parameter set Θ is partitioned into 6 critical regions, as in Fig. 2(b); the blue one consists of all θ that can reduce the curtailment to 0. Among all the candidates in the blue CR, $\theta = [20.8 \text{ MW}, 95.49 \text{ MWh}]$ yields the lowest capital cost of $\$2.53 \times 10^7$, and the energy-power capacity ratio is $E^m/P^{sm} = 4.6$h. The ratio E^m/P^{sm} ranges between $[3, 6]$h in the blue region.

The explicit expression of $v_c(\theta)$ provides great convenience for determining the curtailment. Given a parameter θ, we first locate the specific critical region it resides in, and then the curtailment is an affine function in θ. More importantly, it reveals the sensitivity of renewable energy curtailment to ESU capacity parameters. For example, considering an ESU with $\theta = [40 \text{ MW}, 50 \text{ MWh}]$, the objective function is $v_c(\theta) = 52.9 - 0.56\theta_2 = 24.9$ MWh and is independent of θ_1, implying that the main bottleneck is the energy capacity E^m; improving the power capacity P^{sm} is of little use because there is nowhere to store additional energy. The sensitivity with respect to θ_2 is 0.56, which means the increase of 1 MWh E^m can reduce 0.56 MWh renewable energy curtailment. In fact, the sensitivity
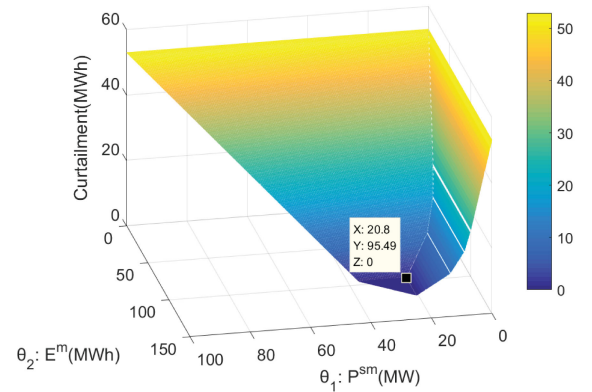
(a) Piecewise linear optimal value function.
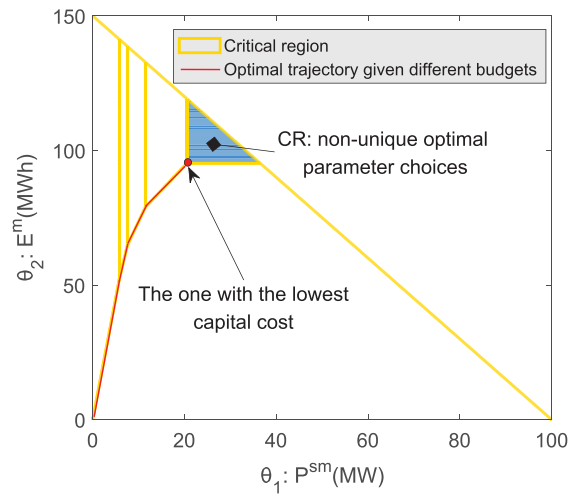
(b) Partition of CRs.

Fig. 2. Visualized results of renewable energy curtailment on 9-bus system.

TABLE I
OPTIMAL PARAMETERS FOR CURTAILMENT REDUCTION ON 9-BUS SYSTEM GIVEN DIFFERENT BUDGETS

Budget($)	Optimal parameters		Curtailment(MWh)	E^m/P^{sm}(h)	SCR(MWh)
	P^{sm}(MW)	E^m(MWh)			
0	0	0	52.92	0	\
0.5×10^7	2.42	21.27	41.09	8.8	11.83
1.0×10^7	4.84	42.54	29.27	8.8	11.83
1.5×10^7	7.26	63.81	17.44	8.8	11.83
2.0×10^7	12.68	80.94	7.96	6.4	9.48
2.5×10^7	20.27	94.58	0.38	4.7	7.58
3.0×10^7	Multiple choices		0	$3 \sim 6$	0.38

information at any point can be seen from equation (20), which can provide useful reference for decision-makers.

Changing the budget from 0 to H_0, the optimal choice of θ moves along the red trajectory plotted in Fig. 2(b). This trajectory divides the parameter set into two subsets; for any point in the above/below subregion, the impact of E^m/P^{sm} is saturated. Sampled points on this trajectory and system performances are summarized in Table I. When the budget is very limited, the ratio E^m/P^{sm} reaches 8.8; it gradually drops as the budget grows. SCR is short for sequential curtailment reduction which means the reduction compared to the previous scenario. We can observe
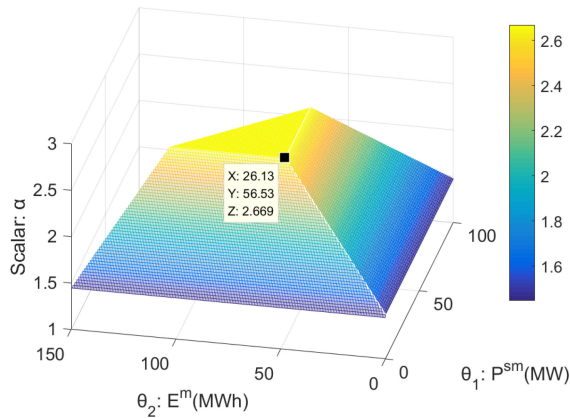
Fig. 3. Optimal value function of uncertainty mitigation on 9-bus system.

TABLE II
IMPACT OF THE INITIAL LEVEL OF SoC ON RENEWABLE ENERGY UTILIZATION

Initial level of SoC		30%	40%	50%	60%	70%
Renewable energy curtailment	P^{sm}(MW)	20.5	20.5	20.8	20.1	19.9
	E^m	68.5	79.9	95.5	119.1	120.1
	Investment cost ($\times 10^7$\$)	1.99	2.21	2.53	3.00	3.00
	Curtailment (MWh)	0	0	0	0.459	11.75
Uncertainty mitigation	P^{sm}(MW)	26.1	26.1	26.1	26.1	26.1
	E^m(MWh)	56.5	56.5	56.5	56.5	56.5
	Investment cost ($\times 10^7$\$)	1.91	1.91	1.91	1.91	1.91
	α	2.67	2.67	2.67	2.67	2.67

TABLE III
VALIDATION OF ALGORITHM 1: THE RESULTS OF CRITICAL SENARIOS
WITH DIFFERENT PARAMETERS

Parameter ([MW,MWh])	Curtailment (MWh)			α		
	ξ_1	ξ_2	ξ_3	ξ_4	ξ_5	ξ_6
$\theta_1 = [0, 0]$	52.9	32.0	12.0	1.44	1.50	1.97
$\theta_2 = [10, 50]$	25.2	0.56	0	1.92	2.08	2.41
$\theta_3 = [30, 75]$	11.1	0	0	2.67	2.67	2.67
$\theta_4 = [70, 25]$	38.9	20.6	0	2.00	2.21	2.67
$\theta_5 = [90, 15]$	44.6	22.4	0	1.80	1.98	2.30

that the marginal cost of reducing REG curtailment increases. Fully utilization of REG may require massive investment.

2) Results of Uncertainty Mitigation: The optimal value function $v_f(\theta)$ is visualized in Fig. 3. Without energy storage, the power system can tolerate renewable power fluctuation confined to set Ξ in (5) with 1.4 h forecast error. When ESU is equipped, with a proper choice of E^m and P^{sm}, α reaches 2.7, manifesting that the flexibility of the power system for uncertainty mitigation is doubled.

From Fig. 3 we can observe that with a sufficient budget, the maximum α is 2.7, bounded by the wind farm capacity. The sizing strategy leading to the maximum α is not unique; $\theta = [26.13 \text{ MW}, 56.53 \text{ MWh}]$ is the one with the minimum capital cost of 19 million dollars, as marked in Fig. 3, and the corresponding energy-power ratio is $E^m/P^{sm} = 2.2$ h. When the budget shrinks, both of E^m and P^{sm} decrease with such a constant ratio. In this test, the ratio E^m/P^{sm} is smaller compared to the result for curtailment reduction, but P^{sm} is even larger, implying that the power capacity of ESU plays a more important role in mitigating short-term uncertainty of wind generation.

By and large, the test on the 9-bus system demonstrates the outcomes of the proposed method and how such outcomes, such as the sensitivity information and the ratio E^m/P^{sm}, can help the decision-maker select a proper storage device.

3) Impact of the Initial Level of SoC: Here we explore how the initial level of SoC impacts the renewable energy utilization. We set E_0 to 30%~70% of E^m with a 10% step size; the results are gathered in Table II. The vector of optimal parameters $\theta = [P^{sm}, E^m]$ achieves the minimum/maximum curtailment/system flexibility.

The impact of the initial level of SoC mainly appears in the renewable energy curtailment subproblem. With the level grows from 30% to 70%, the optimal power capacity is nearly a constant but the energy capacity increases by 75.3%; consequently, the investment cost rises. The reason is that at the early hours, the renewable (wind) energy is rich while the demand is very low; the energy storage helps to utilize the surplus energy at those hours. The initial level of SoC determines how much energy can be stored; given a higher level, a larger energy capacity is needed to provide more storage space; with $E_0 = 60\%$ or $70\%E^m$,

the curtailment cannot be reduced to zero because the energy capacity is limited by the budget. Most importantly, the results show that the ratio E^m/P^{sm} varies from about 3 to 6, which consistent with the conclusion drawn in IV-A1; hence, such a range is universal.

For uncertainty mitigation, energy storage plays a role in providing emergent power support when the demand grows but renewable power drops down, which generally does not happen at night hours. Therefore, the results of the uncertainty mitigation subproblem are independent of the change of the initial level of SoC.

4) Validation of Algorithm 1: In Algorithm 1, we assume that if pattern A of renewable power output is more severe than pattern B for $\theta = 0$, this relation still holds for other values of θ. Such an intuitive assumption is very important for the solution of our proposed model.

To validate the concerned assumption, we use flucutation patterns $(z_i^+, z_i^-), i = 1, \ldots, 6$ and sample parameters $\theta_i, i = 1, \ldots, 5$ from the parameter. With θ_i and (z_i^+, z_i^-), we solve the MILP (8) and (10) for renewable energy curtailment problem and uncertainty mitigation problem, respectively.

All the results are gathered in Table III, showing that the relative severity rank of fluctuation patterns does not change with θ_i. So, at least in this study, the concerned assumption is reasonable.

B. IEEE 118-Bus System

In the modified IEEE 118-bus system, two wind farms with a rated capacity of 600MW connect to the main grid at Bus 35 and Bus 93; each of them is equipped with an ESU (ESU-1 and ESU-2); H_0 is set to $\$1.5 \times 10^8$. Complete data can be found in [42].

TABLE IV
OPTIMUMS OF RENEWABLE ENERGY CURTAILMENT PROBLEM
ON 118-BUS SYSTEM GIVEN DIFFERENT BUDGETS

Budget ($)	$\dfrac{E_1^m(\text{MW})}{P_1^{sm}(\text{MWh})}$: (h)	$\dfrac{E_2^m(\text{MW})}{P_2^{sm}(\text{MWh})}$: (h)	Curtailment (MWh)
$0.5H_0$	$\dfrac{137.7}{33.7} = 4.1$	$\dfrac{134.0}{35.2} = 3.8$	501.7
$0.6H_0$	$\dfrac{179.4}{45.3} = 4.0$	$\dfrac{145.2}{38.3} = 3.8$	427.7
$0.7H_0$	$\dfrac{202.3}{51.9} = 3.9$	$\dfrac{173.1}{47.9} = 3.6$	399.3
$0.8H_0$	$\dfrac{223.7}{61.1} = 3.6$	$\dfrac{195.0}{59.6} = 3.3$	344.7
$0.9H_0$	$\dfrac{223.7}{61.1} = 3.6$	$\dfrac{223.1}{91.0} = 2.5$	307.1
$1.0H_0$	$\dfrac{264.1}{105.7} = 2.5$	$\dfrac{211.0}{77.7} = 2.7$	260.1

1) Results on Renewable Energy Curtailment: Here, the vector θ contains four parameters, i.e. $P_1^{sm}, P_2^{sm}, E_1^m$ and E_2^m. $v_c(\theta)$ and $v_f(\theta)$ can be computed without difficulty. However, for the sake of visualization, we need to reduce the dimension of θ.

To this end, we solve MILP (17) by regarding θ as decision variables with the budget varying from $0.5H_0$ to H_0. The optimums of renewable energy curtailment problem are gathered in Table IV. From $0.5H_0$ to $0.8H_0$, the energy and power capacities of these two ESUs are modestly rising, and the ratio of E^m/P^{sm} slightly drops. From $0.8H_0$ to $0.9H_0$, the strategy is to expand ESU-2; further to H_0, ESU-1 plays a more important role in reducing curtailment; the primary reason is the regional difference in network structure.

In practice, a planner may wish to choose a fixed E^m/P^{sm} ratio in sizing the energy storage. From Table IV, we can see the appropriate ratios for storage units are about $E_1^m/P_1^{sm} = 4$h and $E_2^m/P_2^{sm} = 3.6$h, respectively. So we solve mp-MILP (17) with the above E^m/P^{sm} ratios, so that the dimension of parameter θ reduces to 2, and hence the OVF can be visualized.

With the above fixed ratios, the cost for energy capacity of ESU-1 and ESU-2 are 2.75×10^5 $/ MWh and 2.83×10^5 $/ MWh The optimal value function $v_c(\theta)$ is plotted in Fig. 4(a). Without ESU, the renewable energy curtailment of the 118-bus system is 875.8 MWh; the optimal sizes of the two ESUs are $\theta = [350.0, 189.7]$ MWh, attaining the minimum curtailment of 272.1 MWh with the available budget H_0.

Fig. 4(a) reveals that when the budget approaches to 0, the optimal strategy is to only build ESU-1. The main reason is that a fraction of total curtailment in the first wind farm is attributed to the congestion of transmission lines, and the expansion of ESU can absorb this part of energy. The turning point is $\theta = [97.1, 0]$ MWh, after which the sizes of ESU-1 and ESU-2 should be jointly optimized to assist the power system to utilize wind generation. Furthermore, if we only invest ESU-1/ESU-2, the saturation point arrives at $[363.6, 0]/[0, 273.3]$ MWh and the reduction is $329.2/195.4$ MWh, respectively.

The optimal trajectory plotted in Fig. 4(b) indicates the minimal curtailment and the corresponding parameter choice under
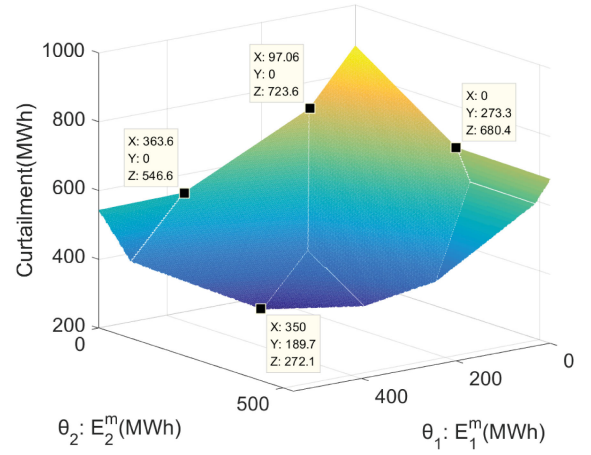
(a) Piecewise linear optimal value function.
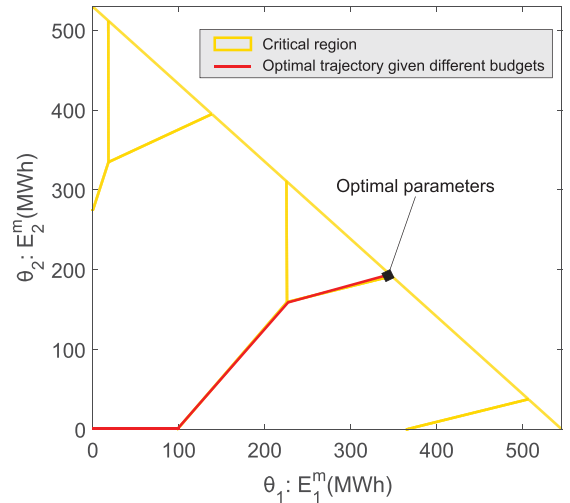
(b) Partition of CRs.

Fig. 4. Visualized results of renewable energy curtailment on 118-bus system with fixed E^m/P^{sm} ratio.

TABLE V
OPTIMUMS FOR CURTAILMENT REDUCTION ON 118-BUS SYSTEM
GIVEN DIFFERENT BUDGETS WITH FIXED E^m/P^{sm} RATIO

Budget($)	E_1^m (MWh)	E_2^m (MWh)	Curtailment (MWh)	Suboptimality
$0.5H_0$	173.6	95.53	520.1	3.7%
$0.6H_0$	198.2	126.1	438.1	2.4%
$0.7H_0$	221.5	155.2	409.2	2.5%
$0.8H_0$	261.1	169.8	361.1	4.8%
$0.9H_0$	304.9	181.8	314.6	2.4%
H_0	350.0	189.7	272.1	4.6%

a given budget. Sampled points are summarized in Table V, providing reference for ESU configuration in practice. The suboptimality in the last column is defined as $(v_c(\theta) - v_c^*(\theta))/v_c^*(\theta)$ where $v_c^*(\theta)$ is the OVF with relaxed ratio of E^m/P^{sm} (please see Table IV) and $v_c(\theta)$ is in Fig. 4(a). The maximum suboptimality is 4.8%; thus, the visualized results in Fig. 4 are qusai-optimal and generally convincing.

2) Results of Uncertainty Mitigation: Similarly, for the problem of uncertainty mitigation, results in Table VI show that

TABLE VI
OPTIMUMS OF UNCERTAINTY MITIGATION PROBLEM ON 118-BUS
SYSTEM GIVEN DIFFERENT BUDGETS

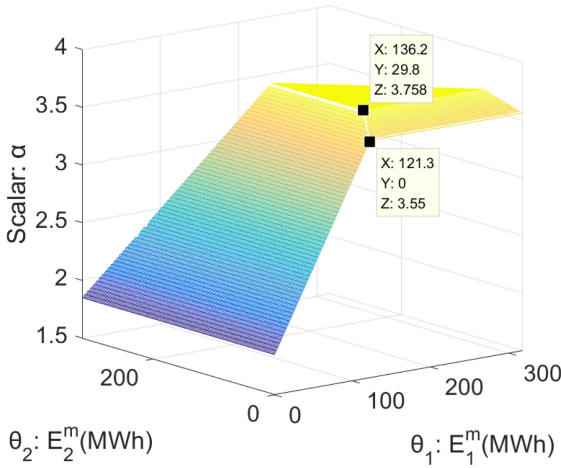| Budget	$\dfrac{E_1^m \text{(MW)}}{P_1^{sm}\text{(MWh)}}$: (h)	$\dfrac{E_2^m \text{(MW)}}{P_2^{sm}\text{(MWh)}}$: (h)	α
$0.1H_0$	$\dfrac{31.9}{28.7} = 1.1$	$\dfrac{0}{0}$	2.3
$0.2H_0$	$\dfrac{63.8}{57.5} = 1.1$	$\dfrac{0}{0}$	2.7
$0.3H_0$	$\dfrac{95.7}{86.2} = 1.1$	$\dfrac{0}{0}$	3.2
$0.4H_0$	$\dfrac{121.3}{110.3} = 1.1$	$\dfrac{4.26}{3.87} = 1.1$	3.5
$0.5H_0$	$\dfrac{132.0}{120.0} = 1.1$	$\dfrac{25.5}{23.2} = 1.1$	3.7
$0.6H_0$	Multiple optimums	Multiple optimums	3.8
$0.7H_0$	Multiple optimums	Multiple optimums	3.8

Fig. 5. Optimal value function uncertainty mitigation on 118-bus system with fixed E^m/P^{sm} ratio.

when the budget is less than $0.4H_0$, ESU-1 is the only choice and the ratio of E_1^m/P_1^{sm} keeps unchanged as 1.1 h; then ESU-2 is invested with the same ratio. Such a ratio is attributed to the role that ESU plays in short-term power support (only one hour in this test); also, it is affected by the discharging efficiency. Multiple optimums are found when the budget is larger than $0.6H_0$ with $\alpha = 3.8$. In view of this, we fix the ratio $E_1^m/P_1^{sm} = E_2^m/P_2^{sm} = 1.1$h for visulization.

With the above fixed ratios, the cost of energy capacity becomes 4.73×10^5\$/ MWh; the optimal value function $v_f(\theta)$ is drawn in Fig. 5. Without ESU, the 118-bus system can tolerate the forecast error αh with $\alpha = 1.8$. The optimal size is $\theta = [136.2, 29.8]$ MWh, which leads to the maximum $\alpha = 3.8$ with the minimum budget of $\$7.85 \times 10^7$.

The information provided by Fig. 5 is consistent with that in Table VI, but more details are revealed. When the budget is relatively low, only the ESU-1 at bus 35 is invested, implying that the reserve capacity in that region is insufficient for higher uncertainty; if the renewable power output drops down by αh,

the demand cannot be served in some periods and load shedding has to be deployed. Hence, the uncertainty of wind farm at bus 35 threats power system security and calls for flexibility resource, which is provided by ESU-1. After the point $\theta = [121.3, 0]$ MWh, the sizes of ESU-1 and ESU-2 should be jointly optimized; with non-unique choices of storage sizes, the flexibility level will hit the ceiling set by the installed capacity of the renewable plant. In this test system, ESU-1 is the key device for uncertainty mitigation, as it possesses a much larger capacity than ESU-2.

C. An Extension Considering the Investment Cost

This paper aims to quantify how the power (MW) and energy (MWh) capacity of ESU would impact renewable energy utilization, which is an evaluation rather than a sizing problem although the parameter set is defined with an investment budget. However, to provide constructive references for ESU planning, it is necessary to incorporate the investment cost into our work. Without injuring the proposed framework in Section II and III, we employ the Nash bargaining criterion to compromise the specific indicator and the investment cost after obtaining the expression of $v_c(\theta)$ and $v_f(\theta)$. Here, we extend the case studies on the 9-bus system to validate this idea.

Taking the renewable energy curtailment problem for example, the curtailment $v_c(\theta)$ and the investment cost $S\theta$ can be regarded as two bargainers; each of which wants to get as far as possible from its worst value; to this end, the Nash Bargain criterion entails solving the following optimization problem:

$$\max \; (v_c(0) - v_c(\theta))(H - S\theta) \quad \text{s.t.} \; \theta \in \Theta \qquad (21)$$

where $v_c(0)$ is the renewable energy curtailment without energy storage. In the objective function of (21), the first term is the curtailment reduction and the second term is the budget surplus; their product is to be maximized; the optimal solution is the bargaining solution, which fairly compromises the curtailment reduction and the investment cost without a manually supplied weight coefficient, which may be subjective.

As discussed in Section IV-A, for a given investment $S\theta$, the optimal choice of θ falls on the optimal trajectory (here denoted by Θ_t) plotted in Fig. 2(b), so does the optimal solution of problem (21). Therefore, we can only consider the parameter points on Θ_t, yielding

$$\max \; (v_c(0) - v_c(\theta))(H - S\theta) \quad \text{s.t.} \; \theta \in \Theta_t \qquad (22)$$

where $v_c(0) = 52.9$ MWh and the budget H is $\$2.53 \times 10^7$, not H_0, which covers the highest cost concerning Θ_t.

To solve (22), we sample 50 points $\theta_i, i = 1, \ldots, 50$ on Θ_t and calculate the corresponding investment $S\theta_i$ and renewable energy curtailment $v_c(\theta_i)$. Then, the diagram of Nash bargaining criterion is drawn in Fig. 6. The breaking point is $(H, v_c(0))$, which indicates the worst outcome of the two objectives; the points are $(S\theta_i, v_c(\theta_i)), i = 1, \ldots, 50$. Problem (22) aims to maximize the area of the shaded rectangle, whose optimal solution is the bargaining solution $(S\theta, v_c(\theta)) = (\$1.24 \times 10^7, 23.2 \text{ MWh})$ and the corresponding storage size is $\theta = [5.9 \text{ MW}, 53.2 \text{ MWh}]$.
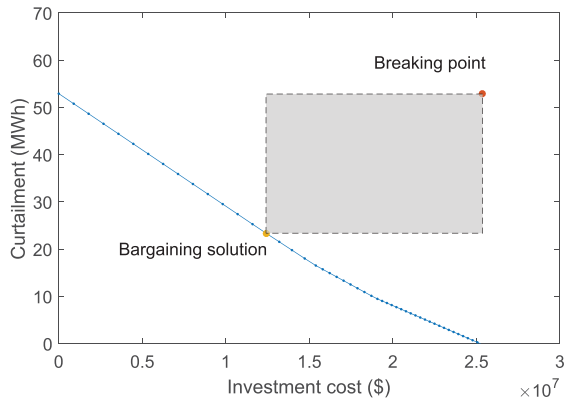
Fig. 6.   Nash bargaining criterion between renewable energy curtailment and investment cost on 9-bus system.
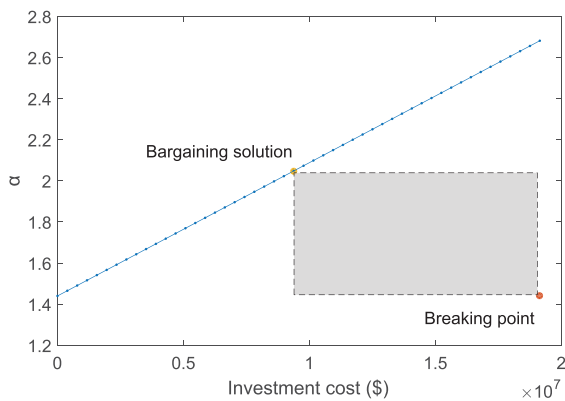

Fig. 7.   Nash bargaining criterion between system flexibility and investment cost on 9-bus system.

Similarly, the Nash bargaining criterion can be employed in the uncertainty mitigation problem. As depicted in Fig. 7, the bargaining solution $(S\theta, \alpha) = (\$9.37 \times 10^6, 2.05)$, giving the storage size of $\theta = [12.8 \text{ MW}, 27.7 \text{ MWh}]$.

In conclusion, the Nash bargaining criterion offers a practical way to compromise the renewable energy curtailment/system flexibility with the investment cost and does not need any subjective weight coefficient, and thus provides constructive references for energy storage sizing.

V. CONCLUSION

This paper proposes two parametric robust optimization models and computational methods to quantify the impact of energy storage on renewable energy utilization in a geometric and visualizable manner. Two indicators reflect the renewable energy curtailment and system flexibility for uncertainty mitigation, which are common concerns of industry.

Abundant sensitivity information can be disclosed by the respective optimal value functions and critical regions; from the perspective of reducing renewable energy curtailment, the proper energy-power ratio of ESU is around 3~6; from the perspective of improving operational flexibility to mitigate short term uncertainty, the reference range of this ratio is about 1~3.

These conclusions, which certainly depend on the specific fluctuation pattern of renewable generation, help system operators make decisions on energy storage sizing considering budget limits, uncertainty, and system security.

Treating other constants as parameters, such as generator and transmission line capacities, the proposed method can investigate how the power system performance/economy is influenced by the chosen parameters, and thus may help make decisions on generation and transmission expansion planning, which is our ongoing work.

REFERENCES

[1] A. Qazi *et al.*, "Towards sustainable energy: A systematic review of renewable energy sources, technologies, and public opinions," *IEEE Access*, vol. 7, pp. 63 837–63 851, 2019.
[2] L. Xie, P. M. S. Carvalho, and L. F. Ferreira, "Wind integration in power systems: Operational challenges and possible solutions," *Proc. IEEE*, vol. 99, no. 1, pp. 214–232, Jan. 2011.
[3] D. J. Burke and M. J. O'Malley, "Factors influencing wind energy curtailment," *IEEE Trans. Sustain. Energy*, vol. 2, no. 2, pp. 185–193, Apr. 2011.
[4] S. Liu, Z. Bie, J. Lin, and X. Wang, "Curtailment of renewable energy in northwest China and market-based solutions," *Energy Policy*, vol. 123, pp. 494–502, Dec. 2018.
[5] M. Black and G. Strbac, "Value of bulk energy storage for managing wind power fluctuations," *IEEE Trans. Energy Conver.*, vol. 22, no. 1, pp. 197–205, Mar. 2007.
[6] R. Jiang, J. Wang, and Y. Guan, "Robust unit commitment with wind power and pumped storage hydro," *IEEE Trans. Power. Syst.*, vol. 27, no. 2, pp. 800–810, May 2012.
[7] S. Adhikari, R. Karki, and P. Piya, "Recovery risk mitigation of wind integrated bulk power system with flywheel energy storage," *IEEE Trans. Power syst.*, vol. 34, no. 5, pp. 3484–3493, Sep. 2019.
[8] Y. Wen, C. Guo, H. Pandi, and D. S. Kirschen, "Enhanced security-constrained unit commitment with emerging utility-scale energy storage," *IEEE Trans. Power Syst.*, vol. 31, no. 1, pp. 651–661, Jan. 2016.
[9] N. Li and K. W. Hedman, "Economic assessment of energy storage in systems with high levels of renewable resources," *IEEE Trans. Sustain. Energy*, vol. 6, no. 3, pp. 1103–1111, Jul. 2015.
[10] S. Wen, H. Lan, Q. Fu, D. C. Yu, and L. Zhang, "Economic allocation for energy storage system considering wind power distribution," *IEEE Trans. Power Syst.*, vol. 30, no. 2, pp. 644–652, Mar. 2015.
[11] L. S. Vargas, G. Bustos-Turu, and F. Larran, "Wind power curtailment and energy storage in transmission congestion management considering power plants ramp rates," *IEEE Trans. Power Syst.*, vol. 30, no. 5, pp. 2498–2506, Sep. 2015.
[12] X. Dui, G. Zhu, and L. Yao, "Two-stage optimization of battery energy storage capacity to decrease wind power curtailment in grid-connected wind farms," *IEEE Trans. Power Syst.*, vol. 33, no. 3, pp. 3296–3305, May 2018.
[13] P. Xiong and C. Singh, "Optimal planning of storage in power systems integrated with wind power generation," *IEEE Trans. Sustain. Energy*, vol. 7, no. 1, pp. 232–240, Jan. 2016.
[14] M. A. Hozouri, A. Abbaspour, M. Fotuhi-Firuzabad, and M. Moeini-Aghtaie, "On the use of pumped storage for wind energy maximization in transmission-constrained power systems," *IEEE Trans. Power Syst.*, vol. 30, no. 2, pp. 1017–1025, Mar. 2015.
[15] D. Pozo, J. Contreras, and E. E. Sauma, "Unit commitment with ideal and generic energy storage units," *IEEE Trans. Power Syst.*, vol. 29, no. 6, pp. 2974–2984, Nov. 2014.
[16] J. Zhao, T. Zheng, and E. Litvinov, "A unified framework for defining and measuring flexibility in power system," *IEEE Trans. Power Syst.*, vol. 31, no. 1, pp. 339–347, Jan. 2016.
[17] K. Bruninx, Y. Dvorkin, E. Delarue, H. Pandžić, W. Dhaeseleer, and D. S. Kirschen, "Coupling pumped hydro energy storage with unit commitment," *IEEE Trans. Sustain. Energy*, vol. 7, no. 2, pp. 786–796, Apr. 2016.
[18] V. Guerrero-Mestre, Y. Dvorkin, R. Fernndez-Blanco, M. A. Ortega-Vazquez, and J. Contreras, "Incorporating energy storage into probabilistic security-constrained unit commitment," *IET Gen. Trans. Distr.*, vol. 12, no. 18, pp. 4206–4215, 2014.

[19] A. Nikoobakht, J. Aghaei, M. Shafie-Khah, and J. P. S. Catalo, "Assessing increased flexibility of energy storage and demand response to accommodate a high penetration of renewable energy sources," *IEEE Trans. Sustain. Energy*, vol. 10, no. 2, pp. 659–669, Apr. 2019.

[20] N. Good and P. Mancarella, "Flexibility in multi-energy communities with electrical and thermal storage: A stochastic, robust approach for multi-service demand response," *IEEE Trans. Smart Grid*, vol. 10, no. 1, pp. 503–513, Jan. 2019.

[21] P. Wang, Z. Gao, and L. B. Tjernberg, "Operational adequacy studies of power systems with wind farms and energy storages," *IEEE Trans. Power Syst.*, vol. 27, no. 4, pp. 2377–2384, Nov. 2012.

[22] Z. Parvini, A. Abbaspour, M. Fotuhi-Firuzabad, and M. Moeini-Aghtaie, "Operational reliability studies of power systems in the presence of energy storage systems," *IEEE Trans. Power Syst.*, vol. 33, no. 4, pp. 3691–3700, Jul. 2018.

[23] Y. Xu and C. Singh, "Power system reliability impact of energy storage integration with intelligent operation strategy," *IEEE Trans. Smart Grid*, vol. 5, no. 2, pp. 1129–1137, Aug. 2013.

[24] J. J. Kelly and P. G. Leahy, "Sizing battery energy storage systems: Using multi-objective optimisation to overcome the investment scale problem of annual worth," *IEEE Trans. Sustain. Energy*, vol. 11, no. 4, pp. 2305–2314, Oct. 2020.

[25] P. Fortenbacher, A. Ulbig, and G. Andersson, "Optimal placement and sizing of distributed battery storage in low voltage grids using receding horizon control strategies," *IEEE Trans. Power Syst.*, vol. 31, no. 3, pp. 2383–2394, May 2018.

[26] Z. Li, Q. Guo, H. Sun, and J. Wang, "Sufficient conditions for exact relaxation of complementarity constraints for storage-concerned economic dispatch," *IEEE Trans. Power Syst.*, vol. 31, no. 2, pp. 1653–1654, Mar. 2016.

[27] H. Bitaraf and S. Rahman, "Reducing curtailed wind energy through energy storage and demand response," *IEEE Trans. Sustain. Energy*, vol. 9, no. 1, pp. 228–236, Jan. 2018.

[28] Z. Yang, H. Zhong, A. Bose, T. Zheng, Q. Xia, and C. Kang, "A linearized OPF model with reactive power and voltage magnitude: A pathway to improve the MW-only DC OPF," *IEEE Trans. Power Syst.*, vol. 33, no. 2, pp. 1734–1745, Mar. 2018.

[29] W. Wei, F. Liu, S. Mei, and Y. Hou, "Robust energy and reserve dispatch under variable renewable generation," *IEEE Trans. Smart Grid*, vol. 6, no. 1, pp. 369–380, Jan. 2016.

[30] W. Wei and J. Wang, *Modeling and Optimization of Interdependent Energy Infrastructures*. Berlin, Germany: Springer, 2020.

[31] S. Boyd and L. Vandenberghe, *Convex Optimization*. Cambridge, UK: Cambridge Univ. Press, 2004.

[32] W. Wei, F. Liu, and S. Mei, "Dispatchable region of the variable wind generation," *IEEE Trans. Power Syst.*, vol. 30, no. 5, pp. 2755–2765, Sep. 2015.

[33] W. Wei, F. Liu, and S. Mei, "Real-time dispatchability of bulk power systems with volatile renewable generations," *IEEE Trans. Sustain. Energy*, vol. 6, no. 3, pp. 738–747, Jul. 2015.

[34] J. E. Falk, "A linear max-min problem," *Math. Program.*, vol. 5, no. 1, pp. 169–188, 1973.

[35] D. Pozo and J. Contreras, "Finding multiple Nash equilibria in pool-based markets: A stochastic EPEC approach," *IEEE Trans. Power Syst.*, vol. 26, no. 3, pp. 1744–1752, Aug. 2011.

[36] V. Dua and E. N. Pistikopoulos, "An algorithm for the solution of multiparametric mixed integer linear programming problems," *Ann. Oper. Res.*, vol. 99, pp. 123–139, 2000.

[37] R. Oberdieck, N. A. Diangelakis, M. Papathanasiou, I. Nascu and E. N. Pistikopoulos, "POP-parametric optimization toolbox," *Ind. Eng. Chem. Res.*, vol. 55, no. 33, pp. 8979–8991, 2016.

[38] Renewables.ninja, 2020. [Online]. Available: https://www.renewables.ninja

[39] D. Bertsimas, E. Litvinov, X. A. Sun, J. Zhao and T. Zheng, "Adaptive robust optimization for the security constrained unit commitment problem," *IEEE Trans. Power Syst.*, vol. 28, no. 1, pp. 52–63, Feb. 2013.

[40] B. Zeng and L. Zhao, "Solving two-stage robust optimization problems using a column-and-constraint generation method," *Oper. Res. Lett.*, vol. 41, pp. 457–461, 2013.

[41] E. Hajipour, M. Bozorg, and M. Fotuhi-Firuzabad, "Stochastic capacity expansion planning of remote microgrids with wind farms and energy storage," *IEEE Trans. Sustain. Energy*, vol. 6, no. 2, pp. 491–498, Apr. 2015.

[42] Z. Guo, "Data-impact of ESU," 2020. [Online]. Available. https://github.com/ZhongjieGuo/Papers

Zhongjie Guo received the B.S. degree from Central South University, Changsha, China, in 2018. He is currently working toward the Ph.D. degree with Tsinghua University, Beijing, China.

His research interests include energy storage, renewable power generation, and power system operation.

Wei Wei (Senior Member, IEEE) received the B.Sc. and Ph.D. degrees in electrical engineering from Tsinghua University, Beijing, China, in 2008 and 2013, respectively.

He was a Postdoctoral Research Associate with Tsinghua University from 2013 to 2015. He was a Visiting Scholar with Cornell University, Ithaca, NY, USA, in 2014, and a Visiting Scholar with Harvard University, Cambridge, MA, USA, in 2015. He is currently an Associate Professor with Tsinghua University. His research interests include applied optimization and energy system economics.

Laijun Chen (Senior Member, IEEE) received the B.S. and Ph.D. degrees in electrical engineering from Tsinghua University, Beijing, China, in 2006 and 2011, respectively. He is currently an Associate Professor with Tsinghua University. His research interests include power system analysis and control, and renewable energy integration.

Zhao Yang Dong (Fellow, IEEE) is currently a Professor in Energy Systems with UNSW, Sydney, NSW, Australia. He is also the Director of UNSW Digital Grid Futures Institute. His research interests includes power system planning and stability, smart grid/micro-grid, load modelling, renewable energy grid connection, electricity market, numerical methods for power system analysis. He served as Ausgrid chair and Director of Ausgrid Centre for Intelligent Electricity Networks to provide R&D support for the Smart Grid, Smart City national demonstration project in Australia. He has been serving/served as Associate Editor for several IEEE transactions and IET journals. He is 2019 highly cited researcher.

Shengwei Mei (Fellow, IEEE) received the B.Sc. degree in mathematics from Xinjiang University, Urumqi, China, in 1984, the M.Sc. degree in operations research from Tsinghua University, Beijing, China, in 1989, and the Ph.D. degree in automatic control from the Chinese Academy of Sciences, Beijing, China, in 1996. He is currently a Professor with Tsinghua University. His research interests include power system complexity and control, game theory, and its application in power systems.